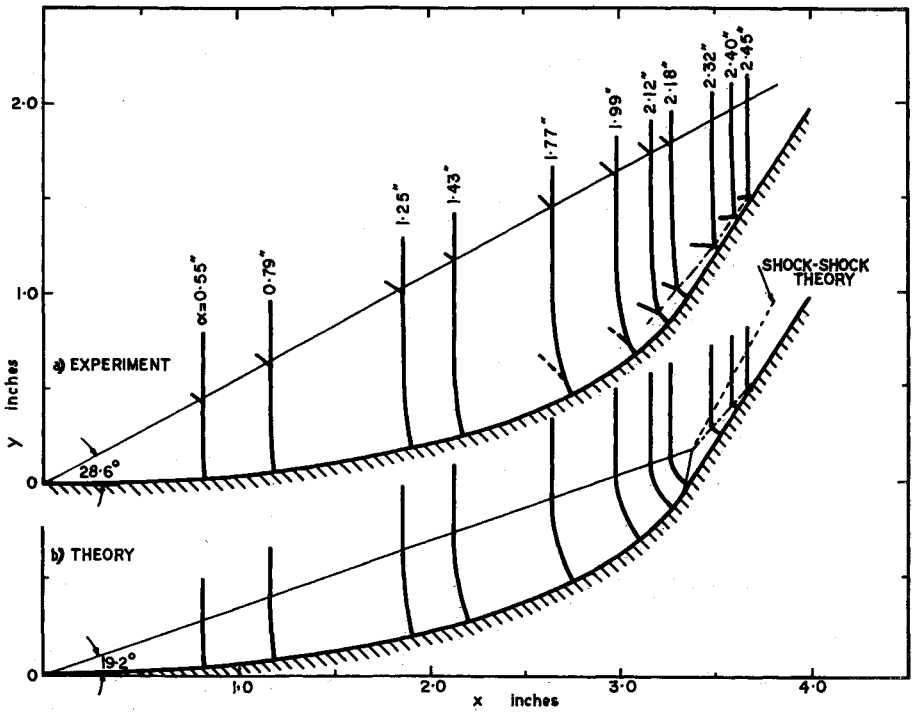

Fig. 4 Theoretical predictions.

Even in the early stages of the process the photographs show a high density gradient immediately behind the shock in proximity to the wall. This compression wave becomes better defined as the shock progresses until at about $\alpha = 2.15$ in. it becomes a reflected shock and a Mach reflection results. This Mach reflection is of the inverted type in that the triple point moves towards the wall and the reflection eventually becomes regular.

The shock-shock shown in Fig. 4b was obtained from geometrical considerations by knowing that the wall shock has a Mach number of 2.2 as predicted from the simple wave theory. On the other hand Whitham's shock-shock theory[3] does not permit the shock-shock to approach the wall as this would permit rays that come from each side of the start of the shock-shock, to intersect. This is inadmissable in the theory. There is thus an anomaly in the end conditions given by the simple wave theory and the conditions required by the shock-shock theory.

The surprising result shown by these tests is that notwithstanding the difference in the starting point of shock curvature nor the noncentred nature of the wave, Whitham's theory gives good agreement as to the position where the shock-shock starts, and as to the position of the shock-shock established on the basis of simple geometrical considerations.

A further interesting point to notice is that the shock curvature is mainly confined to the lower portion of the shock; to such an extent that at $\alpha = 2.45$ in. the shock cannot be distinguished from being plane. Changes in Mach number carried by the upper characteristics of the fan are thus evidently small.

A comparison between the theoretical and experimental shock profiles shows similar effects to previous comparisons for a shock diffracting on plane walls.[5] The experimentally obtained curvature is less than the theoretical so that the part of the shock in contact with the wall is weaker than expected from the theory. These previous tests also showed that the agreement is better for stronger shocks ($M_o > 3.0$) and the same would be expected for shocks shaped in the manner described here.

References

[1] Milton, B. E. and Archer, R. D., "Generation of Implosions by Area Change in a Shock Tube," *AIAA Journal*, Vol. 7, No. 4, April 1969, pp. 779–780.

[2] Lau, J., "Shock Wave Convergence by Wall Shaping," *CASI Transactions*, Vol. 4, 1971, p. 13.

[3] Whitham, G. B., "A New Approach to Problems of Shock Dynamics, Part I," *Journal of Fluid Mechanics*, 2, 1957, p. 145.

[4] Skews, B. W., "Profiles of Diffracting Shock Waves," Rept. 35, Dept. of Mechanical Engineering, Univ. of the Witwatersrand, Johannesburg, South Africa.

[5] Skews, B. W., "The Shape of a Diffracting Shock Wave," *Journal of Fluid Mechanics*, Vol. 29, 1967, p. 297.

Numerical Calculation of Sharp Flat Plate Transitional and Turbulent Skin Friction

J. C. Adams Jr.*
ARO Inc., Arnold Air Force Station, Tenn.

Nomenclature

C_{f_e} = local skin-friction coefficient based on boundary-layer edge conditions, $2\tau_w/\rho_e U_e^2$
M_e = local edge Mach number
$Re_{e,x}$ = local Reynolds number based on boundary-layer edge conditions, $\rho_e U_e x/\mu_e$
T_{aw} = adiabatic wall temperature
T_w = wall temperature
U_e = streamwise velocity at edge of boundary layer
x = surface distance measured from apex of plate
μ_e = viscosity evaluated at boundary-layer edge temperature
ρ_e = density evaluated at boundary-layer edge pressure and temperature
τ_w = wall shearing stress

Received December 20, 1971. This work was sponsored by the Arnold Engineering Development Center (AEDC), Air Force Systems Command (AFSC), U.S. Air Force, under Contract F40600-72-C-0003 with ARO, Inc., Contract Operator, AEDC. Further reproduction is authorized to satisfy needs of the U.S. Government.

* Supervisor, Project Support and Special Studies Section, Aerodynamics Projects Branch, Aerodynamics Division, von Kármán Gas Dynamics Facility. Member AIAA.

Introduction

An accurate analytical method for calculating hypersonic transitional and turbulent heating rates, as well as skin-friction drag, is required for the optimum design of hypersonic re-entry vehicles such as the space transportation system (STS) orbiter. At hypersonic Mach numbers there is great uncertainty and controversy regarding the proper analytical method for calculating turbulent boundary layers under cold wall conditions. Equally important is the choice of criterion for the onset and extent of transition from laminar to turbulent flow. A current state-of-the-art survey of the aerodynamics and aerodynamic heating technology status for STS applications may be found in Ref. 1.

A recent AIAA paper by Hopkins, Keener, and Dwyer[2] was devoted to comparison of calculated turbulent skin friction based on four different classical semiempirical turbulent theories (van Driest, Coles, Sommer, and Short, and Spalding and Chi), as well as a finite-difference integration of the turbulent boundary-layer equations by Dwyer using the eddy-viscosity model of Cebeci,[3] relative to direct measurement (via a floating-element skin-friction balance) on a sharp flat plate for $M_e = 5.9$ to 7.8 at $T_w/T_{aw} \approx 0.3$ and 0.5 in the NASA Ames 3.5-Ft Hypersonic Wind Tunnel. The important conclusion from this investigation was that the van Driest, Coles, and finite-difference theories gave values for the skin friction within about $\pm 10\%$ of the experimental values, but the other theories (Sommer and Short and Spalding and Chi) gave values considerably less than the experiment. However, at very cold wall conditions ($T_w/T_{aw} \approx 0.15$), the investigations by Wallace[4] and Pearce[5] indicate that the Spalding and Chi semiempirical theory yields the most consistently accurate values for both skin friction and heat transfer relative to shock tunnel experimental measurements. Neal[6] recommends use of still another semiempirical theory, Monaghan's T-Prime, based on his experimental study under relatively hot wall ($T_w/T_{aw} \approx 0.50$) conditions. The recent survey paper by Hopkins and Inouye[7] suggests that the semiempirical van Driest II theory be used to predict the turbulent skin friction for the design of supersonic and hypersonic vehicles. The definitive choice of which semiempirical theory evaluated at what reference temperature is most applicable to general hypersonic flows remains an open question.

Recent analytical analyses by Adams[8] and Harris[9] have resulted in development of a laminar, transitional, and turbulent boundary-layer calculation technique based on implicit finite-difference integration of the governing compressible boundary-layer equations using an eddy-viscosity treatment of turbulence in conjunction with an intermittency factor treatment of the transition zone. The objective of the present Note is to show that such calculation techniques are applicable and accurate for sharp flat plate transitional and turbulent skin-friction calculations over a range of wall temperature ratios under hypersonic flow conditions relative to experimental skin-friction measurements reported in Refs. 2, 4, and 6. The report by Adams[8] demonstrates the validity of the present approach for calculation of laminar, transitional, and turbulent heat transfer on sharp cones under hypersonic cold wall conditions. The reader is referred to Ref. 8 for a complete discussion of the method, eddy-viscosity model, and numerical integration technique.

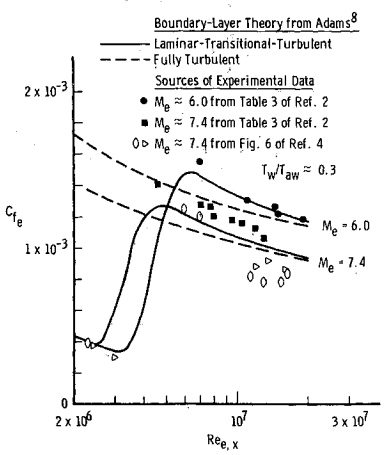

Fig. 1 Skin-friction distributions under relatively cold wall conditions.

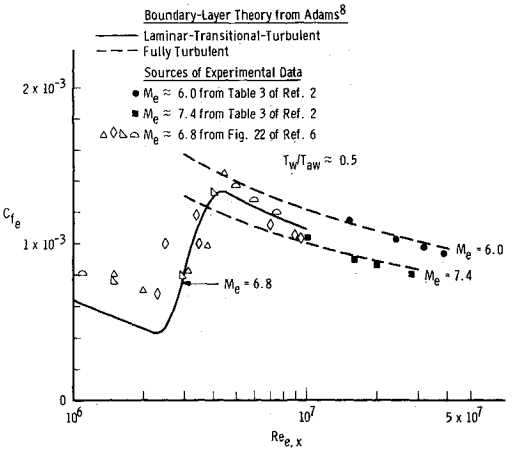

Fig. 2 Skin-friction distributions under relatively hot wall conditions.

Discussion of Results

Figure 1 presents a comparison of calculated laminar, transitional, and turbulent skin friction for a relatively cold wall condition ($T_w/T_{aw} \approx 0.30$) with regard to experimental measurements reported in Refs. 2 and 4. Note the calculated overshoot in skin friction based on the laminar-transitional-turbulent model of Ref. 8 relative to a fully turbulent calculation using the same numerical technique. It should be noted here that the transition model of Ref. 8 requires that the onset of transition be specified a priori; in addition, the ratio of local edge Reynolds number at the end of transition to local edge Reynolds number at the beginning of transition is taken to be two following Masaki and Yakura[10] which, in turn, is used in the intermittency factor treatment of the transition zone. In general, the present calculated results are in good agreement with the experimental data from Ref. 2 except at the peak skin friction denoting the end of transition. The fully turbulent experimental data of Ref. 4 lie some 10–20% below the present calculated results. However, the laminar skin-friction data of Ref. 4 are seen to be in good agreement with the present laminar calculations. The Mach number effect (between $M_e = 6.0$ and $M_e = 7.40$) on the transitional and turbulent skin friction appears to be well-defined by the present analytical method.

A comparison of calculated laminar, transitional, and turbulent skin friction for a relatively hot wall ($T_w/T_{aw} \approx 0.50$) is presented in Fig. 2 with regard to the experimental measurements of Refs. 2 and 6. The laminar skin-friction data of Neal[6] are from 20% to 50% higher than the present laminar calculation (which agrees quite well with the laminar Monaghan T-Prime semiempirical theory used by Neal); the reason for this large discrepancy between theory and experiment in the laminar case is unknown. Again, the transitional and fully turbulent calculated results are in good agreement relative to experiment with the Mach number effect on the transitional and turbulent skin friction well-defined by the present theory.

Presented in Fig. 3 is a comparison of calculated fully turbulent skin friction under hot wall ($T_w/T_{aw} \approx 0.50$) and cold wall ($T_w/T_{aw} \approx 0.15$) conditions relative to the experimental data of Refs. 2 and 4 at a common local edge Mach number of 7.40. Also shown in Fig. 3 is the Spalding-Chi theory for the cold wall condition as taken from Ref. 4. The calculated cold wall skin friction following Adams[8] is some 15 to 20% higher than the Spalding-Chi theory and in reasonable agreement with the experimental data of Ref. 4. Furthermore, the wall temperature effect (between $T_w/T_{aw} \approx 0.15$ and $T_w/T_{aw} \approx 0.50$) on the fully turbulent skin friction appears to be well-defined by the present analytical method and verified by the experimental data. It should be mentioned here that Mayne and Dyer[11] have reported good agreement with the $T_w/T_{aw} \approx 0.15$ fully turbulent skin-

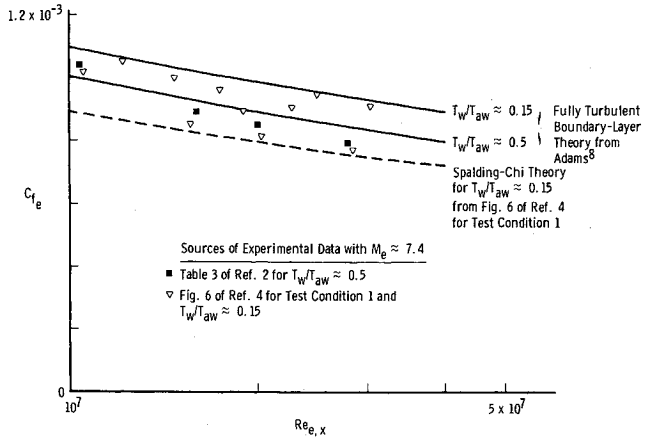

Fig. 3 Effects of wall temperature on skin friction for $M_e = 7.4$.

friction data of Ref. 4 based on application of a modified version of the Patankar-Spalding analysis.[12]

The important point from the above results is that analytical calculation techniques are indeed currently available which can yield valid and accurate values for sharp flat plate transitional and turbulent skin friction over a range of wall temperature ratios under hypersonic conditions, based on numerical integration of the governing boundary-layer equations using an eddy-viscosity model of turbulence and an intermittency factor treatment of transition. Through this approach one is not faced with the question of which semiempirical theory evaluated at what reference temperature is most appropriate for the flow under examination; exactly the same basic analysis is used for all flows.

References

[1] "Space Transportation System Technology Symposium. I-Aerothermodynamics and Configurations," TM X-52876, Vol. I, July 1970, NASA.

[2] Hopkins, E. J., Keener, E. R., and Dwyer, H. A., "Turbulent Skin Friction and Boundary-Layer Profiles Measured on Nonadiabatic Flat Plates at Hypersonic Mach Numbers," AIAA Paper 71-167, New York, 1971.

[3] Cebeci, T., "Calculation of Compressible Turbulent Boundary Layers with Heat and Mass Transfer," *AIAA Journal*, Vol. 9, No. 6, June 1971, pp. 1091–1097.

[4] Wallace, J. E., "Hypersonic Turbulent Boundary-Layer Studies at Cold Wall Conditions," *Proceedings of the 1967 Heat Transfer and Fluid Mechanics Institute*, Stanford University Press, 1967, pp. 427–451.

[5] Pearce, B. E., "A Comparison of Four Simple Calculation Methods for the Compressible Turbulent Boundary Layer on a Flat Plate," *Journal of Spacecraft and Rockets*, Vol. 7, No. 10, Oct. 1970, pp. 1276–1278.

[6] Neal, L., Jr., "A Study of the Pressure, Heat Transfer, and Skin Friction on Sharp and Blunt Flat Plates at Mach 6.8," TN D-3312, April 1966, NASA.

[7] Hopkins, E. J. and Inouye, M., "An Evaluation of Theories for Predicting Turbulent Skin Friction and Heat Transfer on Flat Plates at Supersonic and Hypersonic Mach Numbers," *AIAA Journal*, Vol. 9, No. 6, June 1971, pp. 993–1003.

[8] Adams, J. C., Jr., "Eddy Viscosity-Intermittency Factor Approach to Numerical Calculation of Transitional Heating on Sharp Cones in Hypersonic Flow," TR-70-210 (AD714058), Nov. 1970, Arnold Engineering Development Center, Arnold Air Force Station, Tenn.

[9] Harris, J. E., "Numerical Solution of the Equations for Compressible Laminar, Transitional, and Turbulent Boundary Layers and Comparisons with Experimental Data," TR R-368, Aug. 1971, NASA.

[10] Masaki, M. and Yakura, J., "Transitional Boundary Layer Considerations for the Heating Analysis of Lifting Re-Entry Vehicles," *Journal of Spacecraft and Rockets*, Vol. 6, No. 9, Sept. 1969, pp. 1048–1053.

[11] Mayne, A. W., Jr., and Dyer, D. F., "Comparisons of Theory and Experiment for Turbulent Boundary Layers on Simple Shapes at Hypersonic Conditions," *Proceedings of the 1970 Heat Transfer and Fluid Mechanics Institute*, Stanford University Press, 1970, pp. 168–188.

[12] Patankar, S. V. and Spalding, D. B., *Heat and Mass Transfer in Boundary Layers*, CRC Press, Cleveland, Ohio, 1968.

Structural Averaging of Stresses in the Hybrid Stress Model

JOHN P. WOLF*
Digital Ltd., Zurich, Switzerland

IN the finite-element method using the assumed stress hybrid model,[1,2] the statical behavior of the structural system is governed by the stress-displacement relations [Eq. (1)] and the equilibrium equations [Eq. (2)]

$$H \cdot \beta - T \cdot A^t \cdot u = -\delta o_\beta \tag{1}$$

$$A \cdot T^t \cdot \beta = P \tag{2}$$

where β = (unknown) stress-coefficient vector of all elements, u = (unknown) displacement vector of the nodal points, H = flexibility matrix of all elements, T^t = generalized concentrated force matrix of all elements, A = incidence matrix, δo_β = initial strain vector of all elements, and P = load vector of the nodal points (either applied directly or by premultiplying the "built-in" stress distribution, which has been integrated with the assumed boundary deformation, with the A matrix). In the H and T matrices, the corresponding matrices of the individual elements are assembled on the diagonal. For the sake of simplicity, in Eq. (1) it is assumed that no boundary deformations other than zero are prescribed. Reaction forces and the corresponding zero deformations have been eliminated from Eqs. (1) and (2).

Solving Eqs. (1) and (2), normally on an element basis, the u's and the β's are calculated. The stress distribution is determined from β, adding that of each element regarded as "built-in".[2] The stress field will, in general, exhibit finite discontinuities at the boundaries of each element. To calculate stresses at a nodal point, normally some kind of weighted average of stresses of the neighboring elements is determined. Many averaging procedures used in practice are based on arithmetic or geometrical but not on structural considerations. A review of present methods and a consistent procedure for displacement models are given in Ref. 3.

To average stresses structurally and thus to avoid discontinuities in certain points, additional equilibrium and/or continuity equations are added to Eq. (2) and indirectly also to Eq. (1). These express [Eq. (4b)] that the (final) stresses in certain interelement boundary points, normally where stress results are to be determined, are equal. They are a function of the β's. The modified stress-displacement [Eq. (3)] and equilibrium equations [Eqs. (4a) and (4b)] are

$$H \cdot \beta - T \cdot A^t \cdot u - t \cdot a^t \cdot q = -\delta o_\beta \tag{3}$$

$$A \cdot T^t \cdot \beta = P \tag{4a}$$

$$a \cdot t^t \cdot \beta = p \tag{4b}$$

t^t and a are the coefficient and incidence matrices, respectively. p, the right-hand side of the additional equations, is equal to the sum of the prescribed value (normally zero) and the negative "built-in" values of the neighboring elements, premultiplied by a, q is the vector of the corresponding additional deformations.

To avoid any kinematical deformation modes, the total number of stress modes (length of vector β) must be at least as large as the number of generalized displacements (sum of the lengths of the vectors u and q) after eliminating the rigid-body degrees of freedom of the structure. Care has to be taken to ensure that Eqs. (4a) and (4b) are linearly independent. By choosing the additional equations [Eq. (4b)] in such a way that together with Eq. (4a) the stresses across interelement boundaries are in equilibrium, an equilibrium model is derived. An analogous procedure of formulating additional equilibrium equations can be used to enforce systematically stress-boundary conditions.[4]

Solving Eq. (3) for β and substituting into Eqs. (4a) and (4b), we obtain

$$\beta = H^{-1} \cdot T \cdot A^t \cdot u + H^{-1} \cdot t \cdot a^t \cdot q - H^{-1} \cdot \delta o_\beta \tag{5}$$

Received December 22, 1971.

* Civil Engineer, Structural Department.